

Near-Magnet Power Amplifier with built-in Coil Current Sensing

Klaus Solbach¹, Ashraf Abuelhaija¹, and Samaneh Shoostary¹
¹RF Technology, University Duisburg-Essen, Duisburg, Germany

Purpose:

Presently, commercial 7 Tesla (7T) Magnetic Resonance Imaging (MRI) systems provide only limited numbers of transmit (Tx) channels. Our installation runs a Magnetom 7T MRI system of 8 channels with each 1 kW output power. Since it was found that for whole body imaging the total Tx power is inadequate, an extension is planned employing 32 power amplifiers (PA) of 1kW output power placed near the magnet for efficiency reasons. With the PA near the magnet, the use of circulators / isolators is prohibited leaving the PA output impedance grossly mismatched to 50Ω and the output power and phase varying with the coil impedance and with mutual coupling. However, the close distance between PA and coil also allows compensation of these problems and even an improvement w.r.t. coil decoupling. Several approaches have been published to compensate disadvantages relative to conventional (matched) transmitters, e.g., by Cartesian feedback [1], ultra-low output impedance [2], current-mode class D operation [3] and amplifier balancing [4]. This contribution presents a new concept of a near-magnet PA which closely cooperates with the coil to allow control of the coil current and provide coil decoupling.

Methods and Construction:

The concept of the power amplifier and coil combination is shown in Fig.1. The PA output matching stage is indicated with two probes sampling the output voltage across a quarter-wave transmission line. The PA output is connected to the coil by a tuned (N x half-wavelength) cable while the coil utilizes a quarter-wave transformer as the matching network for a meander dipole coil with balun. For a lossless transmission line transformer, the current I_2 into the dipole coil is proportional to the voltage U_1 at the transformer primary side. Also, this voltage is equal to the probe voltage U_1 at the PA output if the connecting cable can be assumed lossless. Thus, this probe voltage is proportional to the coil current. On the other hand, the probe voltage U_1 is proportional to the voltage at the coil terminals U_2 . Both proportionality constants depend on the probe factor of the probes, and on the characteristic impedance of the quarter-wave transformer. Without the need for an extra field sensor, the probe voltage U_1 can be used to control the coil current, e.g., in a Cartesian feed-back loop as in [1] or [5], effectively creating a current-source. Both probe voltages may be used to check the correct operation of the equipment and guard the SAR limits. From the particular combination of PA and coil it also follows that if the output impedance of the PA is low, the coil is terminated in a high impedance which suppresses current flow from mutual coupling, thus effectively creating transmit amplifier decoupling. The power amplifier prototype is presented in Fig.2(a) with the parts of the shielded cooling cassette disassembled. As one detail, the voltage probe at the PA output is shown in Fig.2(b). The PA employs the MRF6VP41 LDMOS transistor in a balanced final stage and the MRF6V2010 in a driver stage, both supplied with regulated 48 V at the Drain from a capacitor bank as part of the cassette. The voltage probe uses a 22kΩ resistor in combination with a 40 pF shunt capacitor and the 50Ω termination to probe the microstrip line, thus creating a frequency-independent voltage divider of about 54 dB probe attenuation.

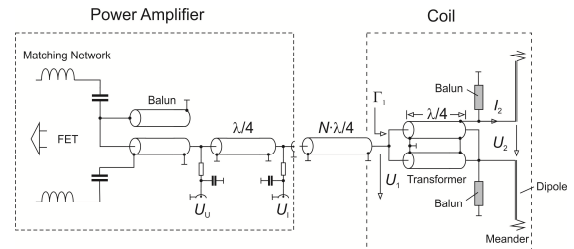


Fig.1: Concept of Power Amplifier with built-in coil current sensing

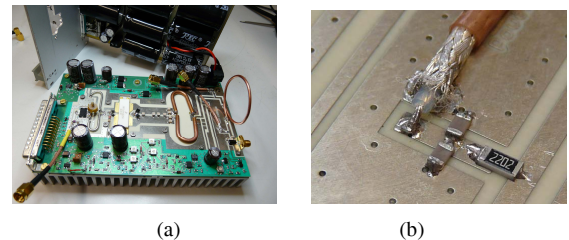


Fig.2: PA board with capacitor bank (a), and voltage probe at the PA output (b)

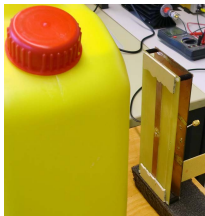


Fig.3: Meander dipole coil close to phantom

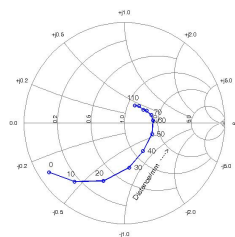


Fig.4: Reflection coefficient of coil as function of distance

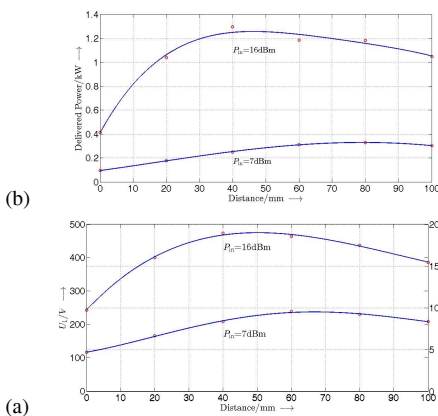


Fig.5: Voltage at the coil input terminals and the coil current as function of distance to the phantom (a) and the resulting calculated delivered power (b)

Results

To demonstrate the function of the PA circuit, a test was performed with a meander dipole coil[6] placed close to a phantom, Fig.3, and connected to the PA with a low-loss cable of 5mm dia. and length 2λ . The PA was driven at full power (16 dBm input) or at reduced power level (7 dBm input) and the probe voltages were measured using an oscilloscope while the distance of the coil to the phantom was increased in steps. The coil reflection coefficient Γ_1 is plotted in Fig.4 as a function of the distance. The corresponding probe voltage U_1 was used to calculate the voltage U_1 at the coil input and the coil current I_2 as shown in Fig.5(a). Using the input voltage U_1 in combination with the coil conductance, the delivered power was calculated and plotted as a function of the coil to phantom distance in Fig.5(b).

Discussion

The PA combination with a coil was successfully used to demonstrate the “remote” sensing of current and voltage at the coil. The measured probe voltages directly relate to the coil current and the delivered power. A magnetic field probe offset from the dipole by several centimetres was used to probe the magnetic field generated by the coil and its variation showed correlation to the measured current at larger distances of the coil to the phantom. For small distances the variation with distance differed considerably which may be due to major changes in the magnetic field distribution around the coil. The critical component in the system seems to be the cable between the PA and the coil: Its effective electrical length has to be precisely met at the operating frequency, and the useful bandwidth reduces with the cable length. Also, the cable attenuation not only reduces the power delivered to the coil but also degrades the measurement accuracy for the coil current – for the intended application cable lengths of about 3 to 4 m are expected to be installed which calls for low-loss cable of 5mm to 10 mm diameter for acceptable measurement accuracy.

References: [1] Hoult D et al, JMR 171 (2004) 64-70, [2] Xu Chu et al, Magn Reson Med 2009; 61:952-961, [3] Gudino N et al, Magn Reson Med 2013; 70(1):276-89, [4] Scott G, Proc. Intl. Soc. Mag. Reson. Med. 20 (2012): 2797, [5] Zanchi M et al, Proc. Intl. Soc. Mag. Reson. Med. 18 (2010): 1465, [6] S. Orzada et al., Proc. Intl. Soc. Mag Reson Med 16 (2008): 2979

Acknowledgement: The research leading to these results has received funding from the European Research Council under the European Union's Seventh Framework Programme (FP/2007-2013) / ERC Grant Agreement n. 291903 MRexcite.